J. Am. Chem. Soc. 1989, 111, 1193−1203

aldehydic C–H bond since very little η^2(C,O) CH_3CO is formed from η^2(C,O) CH_3CDO decomposition but probably that the aliphatic C–H bonds and/or the C–CH_3 bond are weaker than the aliphatic C–D bonds and/or the C–CD_3 bond. This, coupled with the shift in the 350 K peak temperature to 357 K for HD and 367 K for D_2 from CH_3CDO decomposition (Figure 2), indicates a small, but detectable, isotope effect in the decomposition of η^2(C,O) acetaldehyde.

4.2.2. Other Species. As mentioned above, very small amounts of η^2(C,O) CH_3CO are likely in the decomposition of η^2(C,O) CH_3CHO. This species is characterized by coincident desorption of H_2 and CO_2 at 450 K in TPD, CH_3^+, and CH_3CO^+ +SSIMS signals and an intense ν(CO) loss at 1420 cm^{-1}.[5,6] The ν(CO) mode of η^2(C,O) acetyl, produced from η^2(C,O) CH_3CHO decomposition in this study, is not clearly resolved by HREELS because its coverage is low. The CD_3^+ and CD_3CO^+ ions of Figure 7 attenuate coincident with the 448 K D_2 TPD state, indicating that some η^2(C,O) CD_3CO does result from CD_3CDO decomposition.

There is no evidence that η^2(C,O) CH_3CHO decomposition results in CCH_3 formation. The HREELS of CCH_3 should give a loss at 1100 cm^{-1} from the ν(CC) mode[24] but is not observed in Figure 13e from η^2(C,O) CH_3CHO decomposition. CCH_3 formation from CH_3CHO decomposition was observed by McCabe et al. on Pt(S)[6(111)×(100)].[3]

The decomposition of C_xH fragments is responsible for most of the H_2 desorption above 400 K. These fragments result from decomposition of η^2(C,O) CH_3CHO. However, since the amount of H_2 above 400 K is much less than that below 400 K, C_xH is a minority species in CH_3CHO decomposition. An HREELS loss at about 850 cm^{-1} in Figures 10d and 13e is due to the δ(CH) mode of C_xH, and losses in the 1400–1200-cm^{-1} region may be attributed in part to the ν(CC) mode.

5. Summary

A. Surface CH_3CHO Polymerization. HREELS results indicate that low CH_3CHO exposures (<0.4 langmuir) on Ru(001) at 110 K polymerize in two dimensions across the surface. The surface polymer is formed from the reaction of neighboring transiently adsorbed η^1(O) CH_3CHO molecules and decomposes exclusively to η^2(C,O) CH_3CHO at 250 K.

B. η^1(O) CH_3CHO. η^1(O) CH_3CHO is unstable with respect to two-dimensional polymer formation, and it is only observed at exposures near saturation of the first layer and at temperatures below 150 K. Above 150 K the η^1(O) species incorporates into the surface polymer.

C. Multilayer CH_3CHO. Multilayer CH_3CHO appears on Ru(001) for CH_3CHO exposures above 1 langmuir and desorbs in TPD at 150 K.

D. CH_3CHO Polymerization above the Surface. Two additional CH_3CHO TPD states (250 and 310 K) appear in TPD only for CH_3CHO exposures above 1.5 langmuir and do not saturate for a 25-langmuir exposure. These TPD states are associated with +SSIMS ions from dimers and trimers and are attributed to CH_3CHO polymerization in three dimensions above the surface. This polymerization requires a multilayer.

E. η^2(C,O) CH_3CHO. The HREEL spectra after heating CH_3CHO to 300 K resembles that of η^2(C,O) CH_3CHO obtained from ketene hydrogenation on Ru(001).[5] Decomposition of this species accounts for all the CO, H_2, and trace CO_2 observed in TPD. The maximum CH_3CHO decomposition coverage (0.11 ML) is reached after an exposure of about 0.5 langmuir.

Acknowledgment. Support of this work by National Science Foundation Grant CHE8505413 is gratefully acknowledged.

Registry No. CH_3CHO, 75-07-0; Ru, 7440-18-8.

Dimethyl Disulfide: Anion–Molecule Reactions in the Gas Phase at 300 K

Joseph J. Grabowski* and Lijian Zhang

Contribution from the Department of Chemistry, Harvard University, 12 Oxford Street, Cambridge, Massachusetts 02138. *Received July 22, 1988*

Abstract: The thermally equilibrated gas-phase anion–molecule reactions of dimethyl disulfide were examined in a helium bath gas at 0.3 Torr at 300 K by the flowing afterglow technique. All anions more basic than methanethiolate were observed to undergo reaction, but anions less basic than HS^- reacted too slowly to form observable products. Sulfur-centered nucleophiles slightly less basic than methanethiolate were found to undergo thiolate/disulfide interchange. Two bimolecular reaction pathways are proposed to account for the primary reaction products: substitution at sulfur and elimination across the carbon–sulfur bond. The elimination pathway involves initial formation of an ion–dipole complex containing thioformaldehyde and methanethiolate, which subsequently undergoes either addition to give a rearranged thiolate product or dissociation. The primary factor in determining whether an anion gives sulfur substitution or elimination products is the structure of the anion and not the nucleophile base strength. Anions at least as basic as methoxide and in which the charge is localized preferred to react by elimination across the carbon–sulfur bond, while all delocalized carbanion bases strongly preferred substitution at sulfur.

The importance of sulfur, demonstrated by the existence of a vast literature, is due to the variety of valence states for sulfur and sulfur's widespread occurrence in chemistry, in biology, in industry, in agriculture, and in air pollution among others. Limiting a discussion to reduced sulfur compounds would still encompass a variety of classes of molecules and span a number of disciplines from thiol/disulfide interchange reactions of biochemical systems to contributions to acid rain via the atmospheric sulfur cycle to desulfurization of fuel stocks. Narrowing the topic even further, much is now known about the reactivity of disulfides in the condensed phase, with the studies concentrating upon cleavage of the sulfur–sulfur bond. However, much less is understood about the nature of competition between reaction at sulfenyl sites versus carbon sites.

It appeared to us that a gas-phase ion–molecule investigation into the intrinsic chemistry displayed by unsolvated, uncomplexed anions reacting with unsolvated, unaggregated reduced sulfur systems would make an important contribution to efforts to thoroughly understand the chemistry of sulfur in all its applications.[1] By utilizing the techniques and approaches developed for

0002-7863/89/1511-1193$01.50/0

the flowing afterglow technique, kinetic and mechanistic studies under carefully controlled conditions allow one to readily study reactive processes or intermediates, at a well-defined temperature, which are much more difficult to examine in the condensed phase. Yet, enough is now understood about the general parameters of room-temperature gas-phase ion–molecule reactions to begin to relate these data to those from similar reactions executed in the liquid phase.

Dimethyl disulfide was chosen as the prototypical reduced sulfur system for our studies. The gas-phase reactions of anions with dimethyl sulfide have been shown to proceed only by proton transfer with no sign of any displacement process.[2] When the sulfide contains β protons, such as in diethyl sulfide, sufficiently basic anions readily invoke an α',β-elimination in gas-phase interactions.[3] Cyclic thioethers are found to undergo gas-phase reaction with anions by either E2 elimination, α',β-elimination, or S_N2 substitution.[4] In the liquid phase, dimethyl disulfide readily undergoes ionic nucleophilic reaction at sulfur to thiomethoxylate enolates and a large variety of other anions.[5] The alkaline decomposition of organic disulfides is quite complicated[6] and thought to occur by way of an initial nucleophilic displacement of sulfur from sulfur by hydroxide ion to yield a thiolate ion and a sulfenate ion.[7] Dimethyl disulfide is fairly well characterized[8] on the molecular scale. The S–S bond (BDE = 74 ± 2 kcal mol^{-1}, 2.022 ± 0.003 Å) is considerably stronger than the C–S bond (BDE = 57 ± 1.5 kcal mol^{-1}, 1.806 ± 0.002 Å), and the lowest energy conformation has a CSSC dihedral angle of 83.9 ± 0.9°.

In the study reported here, we have allowed a series of anions to react with dimethyl disulfide, in the gas phase, under thermally equilibrated (300 K) reaction conditions, where there are no mitigating factors such as solvent, counterions, or aggregates to perturb the intrinsic chemistry as defined by the anion–dimethyl disulfide system alone. The initial question was to discern if anions react with dimethyl disulfide solely by displacement at sulfur or whether other processes might compete. In the event that competition was observed, we became interested in the factors that define the preferred site of reactivity. The results presented below indicate that for anions more basic than thiolates there are two competing product-forming channels and that the selectivity is defined by the structure and not the energetics (as defined by the basicity) of the anionic nucleophile.

Experimental Section

These experiments were carried out at ambient temperatures (i.e., 300 K) utilizing a recently constructed flowing afterglow[9] (FA) which has been described previously.[10] The total pressure in the reaction region was 0.30 Torr and was established by maintaining a constant volumetric flow rate of helium (7.2 STP L min^{-1}) and utilizing the full pumping capacity of our mechanical booster pumping system (481 L s^{-1} for air at 0.5 Torr). Helium was typically 98% or more of the total gas present in the reaction region, the remainder being composed of various amounts of either the gases used as neutral reactant or the gases used to form the reagent ions. When utilized as the first-formed reactant ions, H_2N^- and CH_3O^- were generated by dissociative electron attachment to ammonia (partial pressure of 0.002 Torr) or methyl nitrite[11] (partial pressure of less than 10^{-4} Torr) directly in the upstream portion of the flowing afterglow. Amide production is quite clean, typically only contaminated by small amounts of HO^- (*m/z* 17), CN^- (*m/z* 26), and the cluster ion $H_2N^-[NH_3]$ (*m/z* 33). Even under conditions optimized for H^- detection (which are significantly different from normal operating conditions), little H^- is observed when generating amide. The initial methoxide signal formed from methyl nitrite is typically contaminated by significant amounts of NO_2^- (*m/z* 46) and $CH_2NO_2^-$ (*m/z* 60). HNO^- does not appear to be a significant problem in the FA when generating methoxide from methyl nitrite, as indistinguishable chemical reactivity results are obtained when methoxide is generated from a variety of sources. Hydroxide ion is cleanly generated in a two-step process by dissociative electron capture of nitrous oxide to give the atomic oxygen anion which is then allowed to react immediately with high-purity methane in an H-atom transfer (0.002 Torr each of N_2O and CH_4).[12] Other reactant ions are formed by exothermic proton transfer from an appropriate neutral to one of the first-formed reactant ions (e.g., $H_2C{=}CHCH_2^-$ from H_2N^- and $H_2C{=}CHCH_3$ or CH_2CN^- from HO^- and CH_3CN). In addition to electron impact ionization of methyl nitrite, CH_3O^- was formed by electron impact ionization of methanol or by chemical reaction of amide ion with methanol; these latter two methods also produced the methoxide–methanol cluster ion (*m/z* 63), which was more of a nuisance in the proton-transfer process.

Neutral reagents are added to the instrument by means of a dedicated glass vacuum system.[10] Liquid samples are handled in round-bottom flasks fit with high-vacuum stopcocks; each sample is subjected to several freeze–pump–thaw cycles to remove dissolved gases. Volumetric flow rates of neutrals are determined by measuring a pressure rise in a calibrated volume. The course of all reactions was examined qualitatively, under pseudo-first-order conditions at fixed reaction time, by taking a complete mass spectrum at each of several different concentrations of the neutral reagent. The quantitative branching ratios reported are those that eliminate any contributions from secondary reactions and are obtained from separate experiments as described below.

Consider the reaction of H_2N^- with CH_3SSCH_3, which in a qualitative experiment is observed to yield two product ions, *m/z* 47 and 93, by parallel pathways (eq 1). Both product ions from the H_2N^- reaction appear to be stable with respect to further reaction under the conditions used (that is, neither *m/z* 47 nor 93 is observed to undergo further reaction with CH_3SSCH_3 under the conditions necessary to just completely quench amide).

$$H_2N^- + CH_3SSCH_3 \begin{cases} \xrightarrow{k_{47}} m/z\,47 + MW = 63 & \text{(1a)} \\ \xrightarrow{k_{93}} m/z\,93 + MW = 17 & \text{(1b)} \end{cases}$$

In eq 1, the observed product ion is indicated by its mass-to-charge (*m/z*) ratio while the molecular weight (MW) of the neutral fragment or fragments necessary to attain mass balance is also displayed. Equation 1 is an apt description of our experimental observations: a primary reactant ion (H_2N^-, *m/z* 16) is generated via a known process (electron impact ionization of ammonia) and is allowed to react with a reagent of known structure. With the exception of detachment processes (which are unimportant here), conservation of charge dictates that a product ion replace each reactant ion. The product ions are detected as their mass-to-charge ratio, but the neutral product(s) are *not* observed. From mass balance, we deduce the MW of the neutral product(s) of a given reaction channel. Additional information about the neutral product must come from thermochemical considerations and related (e.g., isotopic) reactions. For such a system as described in eq 1, where there are no secondary reactions, the concentrations of the ions at any time during the reaction are described by eq 2. In eq 2, $[H_2N^-]_0$

$$[H_2N^-]_0 - [H_2N^-]_t = [P_{47}^-]_t + [P_{93}^-]_t \qquad (2)$$

is the initial amide signal, $[H_2N^-]_t$ is the amount of amide remaining at point *t* in the reaction, and $[P_X^-]_t$ is the amount of product ion *m/z X* at point *t*. The amount of any product ion at any time is some fraction

---

(1) Moran, S.; Ellison, G. B. *J. Phys. Chem.* **1988**, *92*, 1794–1803.

(2) (a) Ingemann, S.; Nibbering, N. M. M. *Can. J. Chem.* **1984**, *62*, 2273–2281. (b) Ingemann, S.; Nibbering, N. M. M. *J. Chem. Soc., Perkin Trans. 2* **1985**, 837–840.

(3) van Berkel, W. W.; de Koning, L. J.; Nibbering, N. M. M. *J. Am. Chem. Soc.* **1987**, *109*, 7602–7608.

(4) de Koning, L. J.; Nibbering, N. M. M. *J. Am. Chem. Soc.* **1988**, *110*, 2066–2073.

(5) March, J. *Advanced Organic Chemistry*, 3rd ed.; Wiley & Sons: New York, 1985.

(6) (a) Danehy, J. P. In *Chemistry of Organic Sulfur Compounds*; Kharasch, N., Meyers, C. Y., Eds.; Pergamon Press Inc.: New York, 1966; Vol. 13, Chapter 13. (b) Parker, A. J.; Kharasch, N. *Chem. Rev.* **1959**, *59*, 583. (c) Fendler, J. H.; Hinze, W. L. *J. Am. Chem. Soc.* **1981**, *103*, 5439–5447.

(7) Danehy, J. P. *Int. J. Sulfur Chem. B* **1971**, *6*, 103–114.

(8) (a) Bond dissociation energies are from: Benson, S. W. *Chem. Rev.* **1978**, *78*, 23–35. (b) Structural parameters are from: Beagley, B.; McAloon, K. T. *Trans. Faraday Soc.* **1971**, *67*, 3216–3222.

(9) (a) Ferguson, E. E.; Fehsenfeld, F. C.; Schmeltekopf, A. L. *Advances in Atomic and Molecular Physics*; Bates, D. R., Estermann, I., Eds.; Academic Press: New York: 1969; Vol. 5, pp 1–56. (b) Fehsenfeld, F. C. *Int. J. Mass Spectrom. Ion Phys.* **1975**, *16*, 151–166. (c) Smith, D.; Adams, N. G. In *Gas Phase Ion Chemistry*; Bowers, M. T., Ed.; Academic Press: Orlando, 1979; Vol. 1, Chapter 1. (d) Graul, S. T.; Squires, R. R. *Mass Spectrom. Rev.* **1988**, *7*, 263–358.

(10) Grabowski, J. J.; Melly, S. J. *Int. J. Mass Spectrom. Ion Processes* **1987**, *81*, 147–164.

(11) Caldwell, G.; Bartmess, J. E. *Org. Mass Spectrom.* **1982**, *17*, 456–457.

(12) Bohme, D. K.; Fehsenfeld, F. C. *Can. J. Chem.* **1969**, *47*, 2715–2717.

Table I. Summary of Observed Results for the Quantitative Investigations of the Reactions of Anions with Dimethyl Disulfide in the Gas Phase at 300 K and 0.30 Torr Total Pressure and Their Correction for Naturally Occurring Isotopic Distributions

anion	fractn yield[a]	m/z	n[b]	formula	isotope factor[c]	product yields,[d] %
H_2N^-	0.344 ± 0.024	47	3	$(CH_3S)^-$	0.9393	33.0
	0.656 ± 0.025	93		$(C_2H_5S_2)^-$	0.8825	67.0
HO^-	0.344 ± 0.002	47	2	$(CH_3S)^-$	0.9393	33.3
	0.029 ± 0.001	63		$(CH_3OS)^-$	0.9371	2.9
	0.063 ± 0.001	65		$(CH_5OS)^-$	0.9368	6.2
	0.560 ± 0.005	93		$(C_2H_5S_2)^-$	0.8825	57.6
$H_2C{=}CHCH_2^-$	0.939 ± 0.044	47	5	$(CH_3S)^-$	0.9393	93.5
	0.061 ± 0.044	93		$(C_2H_5S_2)^-$	0.8825	6.5
CH_3O^-	0.130 ± 0.045	47	4	$(CH_3S)^-$	0.9393	12.4
	0.108 ± 0.013	79		$(C_2H_7OS)^-$	0.9262	10.4
	0.762 ± 0.043	93		$(C_2H_5S_2)^-$	0.8825	77.2
$Ph\bar{C}HCH_3$	0.989 ± 0.002	47	2	$(CH_3S)^-$	0.9393	98.8
	0.011 ± 0.003	93		$(C_2H_5S_2)^-$	0.8825	1.2
CH_2CN^-	0.253 ± 0.016	47	2	$(CH_3S)^-$	0.9393	24.8
	0.747 ± 0.015	86		$(C_3H_4NS)^-$	0.9152	75.2
$CH_3COCH_2^-$	0.178 ± 0.034	47	5	$(CH_3S)^-$	0.9393	17.3
	0.822 ± 0.034	103		$(C_4H_7OS)^-$	0.9060	82.7
$CH_2NO_2^-$	1.000	106	3	$(C_2H_4NO_2S)^-$	0.9210	100.0

[a] Average fractional yield ±1 standard deviation based on observation of only the m/z values listed. [b] Number of independent measurements of the branching ratio. [c] Fraction of the product ion with the given molecular structure that will be detected at the m/z value listed (which is the predominant isotopic peak). These values were calculated from values in the table of the isotopes in ref 14. [d] Yield of the product ion of given molecular formula actually formed in the reaction cited (i.e., corrected to include all naturally occurring isotopic variants). These values are calculated by taking the observed amounts and multiplying them by the inverse of the isotope factor and then renormalizing.

of the amount of amide that has undergone reaction; this fraction, as is shown in eq 3, is defined by the ratio of the rate coefficient for the reaction channel of interest to that of the total rate coefficient for the disappearance of amide. By plotting the normalized, observed ion intensities on the ordinate versus the amount of reagent ion that has been consumed by reaction on the abscissa, we obtain a straight line, the slope of which is the branching ratio (i.e., the relative rate coefficient) for that channel. Examples of such data are shown in Results. For ion–molecule systems that show secondary reactions, defined as the reaction of a product ion (such as m/z 47 or 93) with another molecule of the neutral reagent (such as dimethyl disulfide), the above plots will yield curves that approach linearity at low conversions and that sharply deviate from linearity at high conversions of the reactant ion.[13] A quantitative analysis thus gives the primary product ion yields, free from any contributions due to secondary reactions, and at least qualitative information on any reasonably fast secondary reactions (i.e., one can often identify which secondary reactions are taking place). The primary product ion yields can be considered to be the probability of how a single ion–molecule collision complex fractionates among the various product channels. For the reactions discussed below, we find that secondary reactions are unimportant on the reaction time scale utilized to obtain the primary product distributions. The average correlation coefficient of all the branching ratio plots presented here is 0.9964, and the average error in the slope (eq 3) is 2.2%.

$$[P_X^-]_t = \frac{k_X}{k_{47} + k_{93}} \{[H_2N^-]_0 - [H_2N^-]_t\} \qquad (3)$$

It should be noted that reactions of the product ions with the precursor gas(es) to the reactant ion may not always be revealed by a quantitative analysis such as that discussed above (because the concentration of the precursor gas is not varied during the experiment). This latter concern is checked where necessary, by confirming that changing the identity and/or the amount of the precursor gas to the reactant ion does not affect the identity or yield of product ions.

Before all quantitative measurements of the branching ratios, we actively minimize mass discrimination by monitoring relative peak heights of the low-mass and high-mass product ions while decreasing the resolution of our quadrupole, selecting a final setting where the relative heights no longer change with further decreases in the resolution. We have found that our detection and analysis system, when clean and operated under standard conditions, displays essentially no mass discrimination over the mass range of interest here (that is, for measurements of the reaction of amide, the ratio of m/z 93 to m/z 47 is invariant with mass spectral peak widths of 1–5 amu and with low values of potentials on ion optics). However, when the detection and analysis region is dirty, significant mass discrimination can be found. As an example of the magnitude of the mass discrimination effect, consider the reaction of acetone enolate with dimethyl disulfide (discussed below). Our best estimate of the observed intensities for this reaction are 17.8% m/z 47 and 82.2% m/z 103 (average of five independent measurements) and for which the data collection is done under the minimized mass discrimination conditions discussed above. When we carry out the same measurement with a dirty detection system, with high potentials on critical ion optics, and with a quadrupole resolution that provides nominal base-line separation to above mass 1000, we observe intensities of 65.0% m/z 47 and 35.0% m/z 103. This latter branching ratio reflects not only the intrinsic chemistry but also the relative ability of the detection system to analyze and count the two different ionic products. However, by lowering the resolution of the dirty system, typically to ~5 amu FWHM, and using reasonable potentials on ion optics, we obtain the same results as in the clean system.

As described above, branching ratios are experimentally measured by monitoring the most intense isotopic mass spectral peak for any given ion. The predominant isotope[14] of sulfur is at a molecular mass of 32 amu (95.02% of naturally occurring sulfur) and there are significant populations at 33 (0.75%) and 34 amu (4.21%). Thus, by monitoring only the most intense peak for a sulfur-containing ion, we miss a minimum of 4.96% of that ion. Such errors are exacerbated by the fact that some of the ions we are monitoring contain two sulfurs, while others contain none. The other elements also contain naturally occurring isotopes that can be significant in regard to this work. Thus we take the observed intensities of the major isotopic peaks monitored and correct them for the realization that we are not detecting some percentage of the product ion being monitored. The observed amounts and the fraction of the population of each ion monitored are included in Table I along with the corrected product yields. Also included in Table I are the number of independent branching ratio measurements performed for each reaction. The repeated measurements were done far enough apart in time and under different experimental conditions to give us confidence that no experimental artifacts are contained within the data.

Dimethyl disulfide was obtained from J. T. Baker Chemical Co., and a center cut fraction was obtained from an atmospheric pressure distillation on a 20-cm Vigreux column (bp 109 °C). The ^1H NMR spectrum (Bruker, 300 MHz) in $CDCl_3$ reveals no impurities. GC analysis (Hewlett-Packard Model 5890 with DB-1 column) indicates the sample is at least 99.9% pure.

Results

In the following sections we present the results found for a series of room-temperature investigations in which anionic bases (HA^-) were allowed to react with dimethyl disulfide (nominal MW = 94). The results of the reactions detailed below are partially

---

(13) Anderson, D. R.; Bierbaum, V. M.; DePuy, C. H.; Grabowski, J. J. *Int. J. Mass Spectrom. Ion Phys.* **1983**, *52*, 65–94.

(14) (a) *CRC Handbook of Chemistry and Physics*, 66th ed.; Weast, R. C., Ed.; CRC Press, Inc.: Boca Raton, FL, 1985. (b) de Bievre, P.; Barnes, I. L. *Int. J. Mass Spectrom. Ion Processes* **1985**, *65*, 211–230.

Table II. Summary of Results for the Quantitative Investigations of the Reactions of Anions with Dimethyl Disulfide in the Gas Phase at 300 K and 0.30 Torr Total Pressure

anion (HA^-)	$PA(HA^-)$,[a] kcal mol^{-1}	yield of products,[b] %			
		CH_3S^-	$CH_3S^-(H_2A)$	$CH_3SCH_2S^-$ [c]	CH_3SA^-
H_2N^-	403.6	33	0	67	0
HO^-	390.7	33	6	58	3
$H_2C{=}CHCH_2^-$	390.7	94	0	6	0
CH_3O^-	380.6	12	11	77	0
$Ph\bar{C}HCH_3$	379.8	99	0	1	0
CH_2CN^-	372.9	25	0	0	75
$CH_3COCH_2^-$	369.1	17	0	0	83
$CH_2NO_2^-$	356.4	0	0	0	100

[a] Reference 15. [b] See Table I. [c] See text for a discussion of the structures of the various ions and how they were determined.

summarized in Table II, which contains only the quantitative aspects of the study. Unless otherwise indicated, all gas-phase acidity values ($\Delta H°_{acid}[AH]$, the enthalpy of the gas-phase heterolytic dissociation of AH to A^- and H^+, is the same absolute value as the proton affinity of A^-, $PA[A^-]$) cited in this work are from the standard compilations.[15] For those cases where we report "no reaction", it is more proper to say that neither product ions from any reaction nor a decrease in the reactant ion signal is observed within the time window of our instrumental technique. We estimate that we can measure rate coefficients that are greater than or equal to $\sim 1 \times 10^{-13}$ cm^3 $particle^{-1}$ s^{-1} (the maximum rate coefficient is that of the collision frequency which for the systems examined here ranges from 1.94×10^{-9} to 3.37×10^{-9} cm^3 $particle^{-1}$ s^{-1})[16] and that we can qualitatively observe some products from reactions that proceed with rate coefficients greater than 1×10^{-14} cm^3 $particle^{-1}$ s^{-1}.

To determine how reliably we can actually measure relative ion intensities, we made M, M + 1, and M + 2 measurements on the *m/z* 93 ion formed in the reaction of H_2N^- with dimethyl disulfide (see below). For these measurements, we set the quadrupole resolution to the minimum value that gave base-line separation between the M/(M + 1) and the (M + 1)/(M + 2) peaks and that corresponds to FWHM of ~1 amu and kept all critical ion optics at low potentials. The relative intensities of *m/z* 93 to *m/z* 94 to *m/z* 95 observed are 1.0000:0.0363:0.0882, in reasonable agreement with that expected[17] of 1.0000:0.0380:0.0885 for a molecular formula of $C_2H_5S_2$. Based on such measurements, our accuracy is probably ±0.3% on any individual branching ratio measurement. The individual branching ratio measurements that are made under the conditions described above are reproducible, the differences for any reaction channel between measurements often made weeks apart is often less than 2% and back-to-back measurements are reproducible to 0.2%. A conservative estimate places the average error in the reported relative rate coefficients (branching ratio) at 5%.

Amide ($PA[H_2N^-]$ = 403.6 kcal mol^{-1}) is observed to be rapidly quenched upon addition of dimethyl disulfide, being replaced by two product ions, *m/z* 47 and 93, as is summarized in eq 4. Three

$$\underset{m/z\ 16}{H_2N^-} + CH_3SSCH_3 \longrightarrow 33\%\ \underset{m/z\ 47}{CH_3S^-} + [CH_5NS] \qquad (4a)$$

$$\underset{m/z\ 16}{H_2N^-} + CH_3SSCH_3 \longrightarrow 67\%\ \underset{m/z\ 93}{(C_2H_5S_2)^-} + NH_3 \qquad (4b)$$

independent measurements of the branching ratio (the first of which is shown in Figure 1) for this reaction gives 33.3%, 32.9%, and 37.2% CH_3S^- in addition to 66.7%, 67.1%, and 62.8% $(C_2H_5S_2)^-$, which are averaged to yield 34.4 ± 2.4% CH_3S^- and 65.6 ± 2.4% $(C_2H_5S_2)^-$. The bracket about the neutral product of eq 4a (and elsewhere throughout the paper) is to indicate that the chemical structure of the neutral component of the reaction products is not yet stipulated. Likewise, the parentheses around the chemical formula for the *m/z* 93 ion indicates that the ion structure is as yet unspecified. While there can be no doubt as to the structure of the ion at *m/z* 47 or the chemical composition of the ion at *m/z* 93, the neutral product(s) of the first channel (CH_3SNH_2 versus $H_2C{=}S + NH_3$) and the structure of the *m/z* 93 ion (e.g., $CH_3SSCH_2^-$ or other) are not obvious from this one experiment. We shall return to the question of the identity of the *m/z* 93 ion from an experimental standpoint and to the question of the neutral product(s) from an interpretative standpoint. Finally, a primary ion at *m/z* 64, $CH_3S^-(NH_3)$, is not observed.

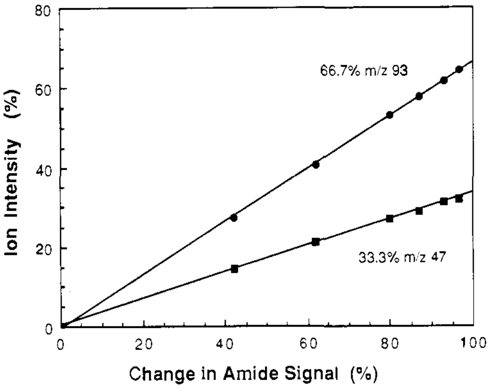

Figure 1. Representative example of a branching ratio plot for the reaction of amide with dimethyl disulfide. The data points are plotted as described in the text; the best fit straight line through the observed data points is that described by eq 3. The average of three independent measurements gives a final observed amount of 34.4% *m/z* 47 and 65.6% *m/z* 93.

In addition to the primary reactions reported above, two ions resulting from secondary chemical reactions are observed but only upon addition of high concentrations of dimethyl disulfide (i.e., they are formed in secondary processes but with small rate coefficients). The two secondary product ions are *m/z* 141, which presumably is the solvated or cluster ion $CH_3S^-(CH_3SSCH_3)$ and *m/z* 79, which is CH_3SS^-. Under the most forcing of conditions, the former accounts for ca. 8% and the latter ca. 2% of the sum of the four primary and secondary product ions (*m/z* 47, 79, 93, and 141). The *m/z* 141 secondary product ion most likely arises from a slow, termolecular clustering reaction between CH_3S^- and CH_3SSCH_3. Studies using carefully synthesized and purified CD_3SSCD_3 have shown that $CH_3CH_2S^-$ reacts to give only CD_3S^-; no CD_3SS^- is detected.[18] Therefore we feel that the CH_3SS^- detected as a trace secondary product in many of the systems reported here is due to a trace impurity, perhaps from the trisulfide or methyl hydrogen disulfide, although no impurity is observed in either the GC or NMR traces.

Hydroxide ($PA[HO^-]$ = 390.7 kcal mol^{-1}) is observed to be rapidly quenched upon addition of dimethyl disulfide, forming

---

(15) (a) Lias, S. G.; Bartmess, J. E.; Liebman, J. F.; Holmes, J. L.; Levin, R. D.; Mallard, W. G. *J. Phys. Chem. Ref. Data* **1988**, *17*, Suppl. 1. (b) Bartmess, J. E.; McIver, R. T., Jr. In *Gas Phase Ion Chemistry*; Bowers, M. T., Ed.; Academic Press: New York, 1984; Vol. 2, Chapter 11.

(16) Collision rate coefficients calculated according to: Su, T.; Chesnavich, W. J. *J. Chem. Phys.* **1982**, *76*, 5183–5185.

(17) Expected M + 1 and M + 2 intensities are calculated by using isotopic abundance tables in ref 14.

(18) Grabowski, J. J.; Zhang, L., unpublished results.

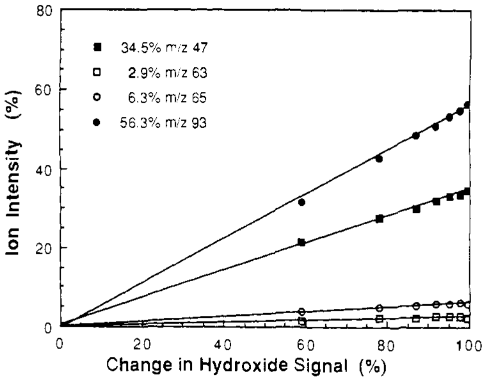

Figure 2. Representative example of a branching ratio plot for the reaction of hydroxide with dimethyl disulfide. The data points are plotted as described in the text; the best fit straight line through the observed data points is that described by eq 3. The average of two independent measurements gives a final observed amount of 34.4% *m/z* 47, 2.9% *m/z* 63, 6.3% *m/z* 65, and 56.0% *m/z* 93.

four product ions, *m/z* 47, 63, 65 and 93, as is summarized in eq 5, while one of the two data sets averaged to give the reported branching ratio is displayed in Figure 2. The same slow secondary processes are detected in the hydroxide system as are detected in the amide system.

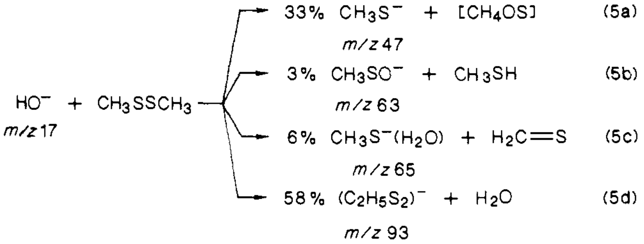

$$HO^- + CH_3SSCH_3 \; (m/z\,17) \rightarrow 33\%\; CH_3S^- \,(m/z\,47) + [CH_4OS] \quad (5a)$$
$$\rightarrow 3\%\; CH_3SO^- \,(m/z\,63) + CH_3SH \quad (5b)$$
$$\rightarrow 6\%\; CH_3S^-(H_2O) \,(m/z\,65) + H_2C{=}S \quad (5c)$$
$$\rightarrow 58\%\; (C_2H_5S_2)^- \,(m/z\,93) + H_2O \quad (5d)$$

Allyl anion (PA[$H_2C{=}CHCH_2^-$] = 390.7 kcal mol^{-1}), as was observed for amide and hydroxide, displays a rapid reaction with dimethyl disulfide, but in this case, only two product ions are observed (eq 6; the yields shown are the average of five independent measurements). Also, as was observed for amide and hydroxide ions, the only secondary products are those at *m/z* 141 and 79, both formed slowly (i.e., present in small concentrations) and with the higher mass ion being ~4 times as abundant as the lower mass ion.

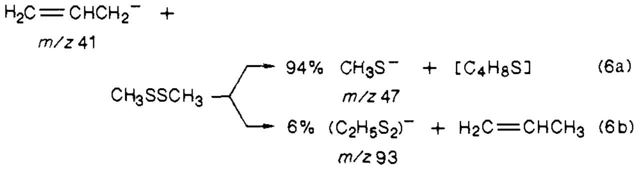

$$H_2C{=}CHCH_2^- \,(m/z\,41) + CH_3SSCH_3 \rightarrow 94\%\; CH_3S^- \,(m/z\,47) + [C_4H_8S] \quad (6a)$$
$$\rightarrow 6\%\; (C_2H_5S_2)^- \,(m/z\,93) + H_2C{=}CHCH_3 \quad (6b)$$

Benzyl anion (PA[$C_6H_5CH_2^-$] = 380.8 kcal mol^{-1}) reacts quite rapidly with dimethyl disulfide to give nearly quantitative amounts of CH_3S^- with just a trace of *m/z* 93. Unfortunately, we are unable to exactly measure this branching ratio; under the low-resolution conditions necessary to confirm that mass discrimination has indeed been minimized, the benzyl anion signal (*m/z* 91) interferes with the $(C_2H_5S_2)^-$ signal (*m/z* 93). As was noted previously for other systems, the two secondary ions *m/z* 141 and 79 are formed slowly, with $CH_3S^-(CH_3SSCH_3)$ predominating.

Methoxide (PA[CH_3O^-] = 380.6 kcal mol^{-1}), when allowed to react with dimethyl disulfide, proceeds in a rapid fashion to yield three product ions as illustrated in eq 7 (average of four measurements). Results of ion–molecule reaction between methoxide and dimethyl disulfide are found to be independent of the source of the reactant methoxide ion.

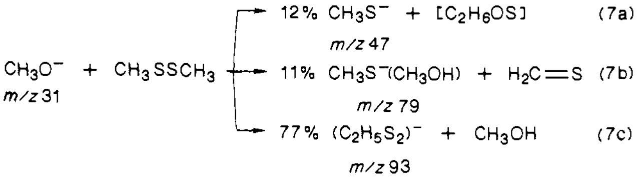

$$CH_3O^- \,(m/z\,31) + CH_3SSCH_3 \rightarrow 12\%\; CH_3S^- \,(m/z\,47) + [C_2H_6OS] \quad (7a)$$
$$\rightarrow 11\%\; CH_3S^-(CH_3OH) \,(m/z\,79) + H_2C{=}S \quad (7b)$$
$$\rightarrow 77\%\; (C_2H_5S_2)^- \,(m/z\,93) + CH_3OH \quad (7c)$$

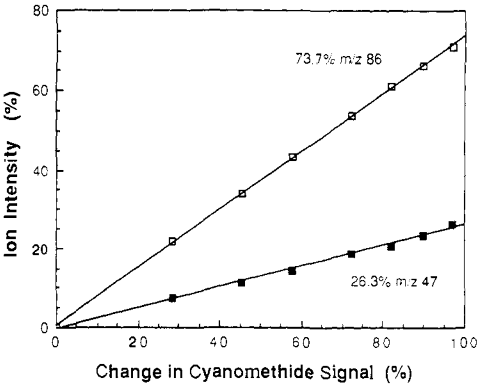

Figure 3. Representative example of a branching ratio plot for the reaction of the conjugate base of acetonitrile with dimethyl disulfide. The data points are plotted as described in the text; the best fit straight line through the observed data points is that described by eq 3. The average of two independent measurements gives a final observed amount of 25.3% *m/z* 47 and 74.7% *m/z* 86.

The ion observed at *m/z* 79 could have the structure shown in eq 7b or it could be CH_3SS^-. We have assigned the ion observed at *m/z* 79 to the methanethiolate–methanol cluster ion, formed in a primary process, on the basis of several observations. First, the yield of *m/z* 79 is independent of the source of methoxide (electron impact on methyl nitrite or methanol; proton abstraction from methanol) and therefore is independent of the amount of methanol present in the reaction region. Second, an ion at *m/z* 79 is not observed as a primary product ion for any other anionic reactant examined here with dimethyl disulfide. In particular, no detectable amount (conservatively, we should be able to detect product ions with yields of at least 0.1%) of *m/z* 79 is observed to be formed in the reaction of ethoxide ion with dimethyl disulfide. Third, isotopic measurements of *m/z* 79, 80, and 81 gave the observed ratio of 1.0000:0.0341:0.0497, which is in agreement with that expected for the cluster ion $CH_3S^-(CH_3OH)$, 1.0000:0.0309:0.0467, and not in accord with that expected for CH_3SS^-, 1.0000:0.0269:0.0882. Finally, the *m/z* 79 ion formed in the methoxide–dimethyl disulfide reaction (eq 7b, methoxide from methyl nitrite) was allowed to react with methanol-*O-d* and observed to give only *m/z* 80 in a fast process. If the *m/z* 79 ion is CH_3SS^-, no reaction with methanol-*O-d* is expected; if the *m/z* 79 ion is $CH_3S^-(CH_3OH)$, fast conversion to $CH_3S^-(CH_3OD)$, *m/z* 80, is expected either by solvent switching or by H/D exchange. Finally, as methanethiol is 23.7 kcal mol^{-1} stronger as a Brønsted acid than is methanol, we write the cluster ion in eq 7b as the thiolate–alcohol form rather than as the alkoxide–thiol.

The conjugate base of ethylbenzene (PA[$Ph\bar{C}HCH_3$] = 379.8 kcal mol^{-1}) rapidly reacts with dimethyl disulfide in a reaction very similar to that of the benzyl anion in that it gives almost quantitatively methanethiolate (eq 8; average of two measurements). In the case of the conjugate base of ethyl benzene, however, we can quantitatively determine the branching ratio as $Ph\bar{C}HCH_3$ is observed at *m/z* 105 which, even under our extremely low resolution conditions, does not interefere with observation of the *m/z* 93 product ion.

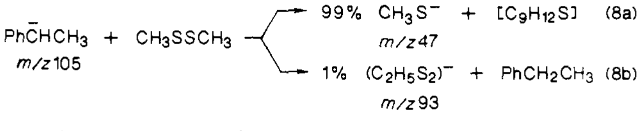

$$Ph\bar{C}HCH_3 \,(m/z\,105) + CH_3SSCH_3 \rightarrow 99\%\; CH_3S^- \,(m/z\,47) + [C_9H_{12}S] \quad (8a)$$
$$\rightarrow 1\%\; (C_2H_5S_2)^- \,(m/z\,93) + PhCH_2CH_3 \quad (8b)$$

The conjugate base of acetonitrile (PA[CH_2CN^-] = 372.9 kcal mol^{-1}) reacts with dimethyl disulfide with a moderate rate to yield two ionic products (eq 9; average of two measurements, one of

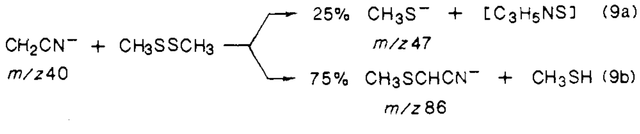

$$CH_2CN^- \,(m/z\,40) + CH_3SSCH_3 \rightarrow 25\%\; CH_3S^- \,(m/z\,47) + [C_3H_5NS] \quad (9a)$$
$$\rightarrow 75\%\; CH_3SCHCN^- \,(m/z\,86) + CH_3SH \quad (9b)$$

which is shown in Figure 3). It is important to note that no *m/z* 93 is detected and that the *m/z* 86 ion corresponds to a product channel not observed for any of the ions reported above.

The most important secondary reaction in the acetonitrile system is reaction of the *m/z* 86 primary product ion with another molecule of dimethyl disulfide, giving a secondary product ion at *m/z* 132. The secondary reaction detected (eq 10) can be

$$\underset{m/z\ 86}{CH_3SCHCN^-} + CH_3SSCH_3 \rightarrow \underset{m/z\ 132}{(CH_3S)_2CCN^-} + CH_3SH \qquad (10)$$

considered to be analogous to the primary process shown in eq 9b. This secondary reaction must have an appreciable rate, as it is possible to completely quench the initial product ion, *m/z* 86, by further addition of dimethyl disulfide. However, the secondary reaction is still considerably slower than the initial reaction. From data collected during our measurements on the primary reaction (eq 9) we are able to identify the secondary reaction shown in eq 10; however, we can not rule out that some small portion ($\leq 5\%$) of the room-temperature collisions between CH_3SCHCN^- and CH_3SSCH_3 forms CH_3S^- instead of *m/z* 132. The secondary reaction shown in eq 10 is considerably more efficient that the secondary reactions producing *m/z* 79 and 141 discussed above.

Acetone enolate ($PA[CH_3COCH_2^-] = 369.1$ kcal mol^{-1}) also reacts with dimethyl disulfide with a moderate rate to give results (eq 11; average of five measurements) similar to those for acetonitrile.

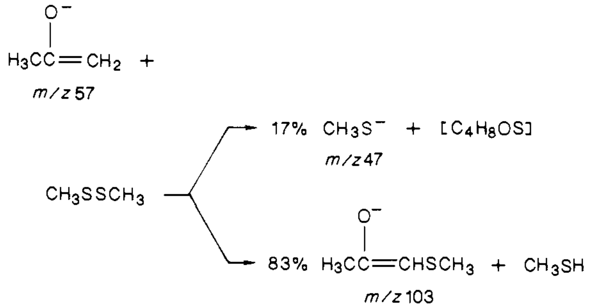

(11a)

(11b)

The predominant secondary reaction in the acetone system is reaction of the major primary product ion, *m/z* 103, with another molecule of dimethyl disulfide to yield *m/z* 149 (eq 12), a process analogous to that observed in the acetonitrile system

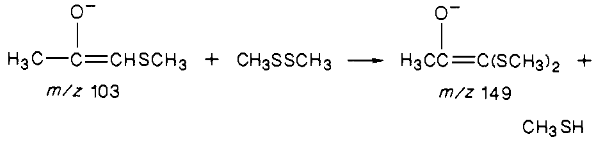

$$\underset{m/z\ 103}{H_3C\overset{O^-}{C}{=}CHSCH_3} + CH_3SSCH_3 \rightarrow \underset{m/z\ 149}{H_3C\overset{O^-}{C}{=}C(SCH_3)_2} + CH_3SH \qquad (12)$$

(i.e., eq 10). The product shown in eq 12 accounts for at least 95% of the secondary reaction of the *m/z* 103 ion. Because this secondary reaction is reasonably slow, our data collected for the primary reaction (eq 11) does not allow us to eliminate a minor ($\leq 5\%$) secondary channel that produces CH_3S^-.

Nitromethide anion ($PA[CH_2NO_2^-] = 356.4$ kcal mol^{-1}) slowly, but completely, reacts with dimethyl disulfide to give, as the sole primary product, an ion at *m/z* 106.

$$\underset{m/z\ 60}{CH_2NO_2^-} + CH_3SSCH_3 \rightarrow 100\%\ \underset{m/z\ 106}{CH_3SCHNO_2^-} + CH_3SH \qquad (13)$$

The only secondary reactions detected in this system are clustering reactions by nitromethane, which are probably due to the large dipole moment ($\mu_D = 3.46$ D) and polarizability ($\alpha = 7.37 \times 10^{-24}$ cm^3) of nitromethane.[19] The secondary reactions observed for acetonitrile and acetone systems are not detected here.

Thioethoxide ($PA[CH_3CH_2S^-] = 355.2$ kcal mol^{-1}) and **thiobutoxide** ($PA[CH_3CH_2CH_2CH_2S^-] = 353.7$ kcal mol^{-1}) do react, albeit extremely slowly, (we are unable to quench more than about $^1/_3$ of the initial thioalkoxide signal) with dimethyl disulfide, giving CH_3S^- as the exclusive product ion.

$$RS^- + CH_3SSCH_3 \rightarrow \underset{m/z\ 47}{CH_3S^-} + RSSCH_3 \qquad (14)$$

The conjugate bases of hydrogen sulfide ($PA[HS^-] = 351.2$ kcal mol^{-1}) and **methyl malonate** ($PA[(CH_3O_2C)_2CH^-] \sim 349$ kcal mol^{-1}) do not appear to react with dimethyl disulfide under the conditions for which the other reactions were examined.

The buffer gas pressure appears to have no effect on the branching ratios reported above. In qualitative experiments, both amide and hydroxide gave the same product distributions at a flow tube pressure of 0.58 Torr (helium; flow rate of 15.3 STP L min^{-1}). In a single, quantitative measurement, we observed methoxide (generated by dissociative electron attachment to methanol) react with dimethyl disulfide to yield 5% CH_3S^-; 11% $CH_3S^-(HOCH_3)$, and 82% $CH_3SCH_2S^-$. The observed yield at the higher bath gas pressure for methoxide is in good agreement with the data already presented at 0.3 Torr.

The *m/z* 93 anion, which has the molecular formula $(C_2H_5S_2)^-$, produced most abundantly in the reaction of methoxide with dimethyl disulfide and to lesser extents with other anions as reported above, could have one of several structures. The two structures that have the most reasonable mechanistic possibilities arising from anionic reactions with dimethyl disulfide are $CH_3SSCH_2^-$ (carbanion form) and $CH_3SCH_2S^-$ (thiolate form). A third possibility is $CH_3CH_2SS^-$ (disulfide form), which might be expected to arise from a diethyl disulfide or a methyl ethyl disulfide impurity. We are able to rule out a diethyl disulfide or a methyl ethyl disulfide impurity based on the absence of ethyl signals in the NMR and the appropriate peaks in the GC trace of the dimethyl disulfide sample and because the ion chemistry of diethyl disulfide gives unique products[18] which are not detected (even in trace amounts) in the dimethyl disulfide experiments. To distinguish between the carbanion and thiolate forms of the *m/z* 93 ion, its chemical reactivity was compared to that of model ions. The conjugate base of dimethyl sulfide, readily prepared by proton abstraction by amide ion (eq 15),[2] was used to model the expected

$$\underset{m/z\ 16}{H_2N^-} + CH_3SCH_3 \rightarrow 100\%\ \underset{m/z\ 61}{CH_3SCH_2^-} + NH_3 + 10.5 \text{ kcal mol}^{-1} \qquad (15)$$

$$\underset{m/z\ 16}{H_2N^-} + CH_3SH \rightarrow 100\%\ \underset{m/z\ 47}{CH_3S^-} + NH_3 + 46.8 \text{ kcal mol}^{-1} \qquad (16)$$

reactivity of the carbanion form of *m/z* 93, while methyl thiolate (eq 16) was used to model the thiolate form. Both reactions 15 and 16 are rapid, exothermic proton transfers. A number of reactions of CH_3S^-, $CH_3SCH_2^-$, and the *m/z* 93 generated by anion reaction with dimethyl disulfide were qualitatively examined and are summarized in Table III, the most salient of which are further amplified here. During these studies, we noted that the chemistry displayed by the *m/z* 93 ion with the reagents listed in Table III was independent of the initial reactant ion used to prepare *m/z* 93. We interpret this consistent chemical reactivity as the same *m/z* 93 ion being formed in all reactions. The model carbanion, $CH_3SCH_2^-$, reacts with D_2O by H/D exchange and by equilibration, while the model thiolate ion, CH_3S^-, is unreactive toward D_2O. The *m/z* 93 ion generated in our dimethyl disulfide reaction is also unreactive toward D_2O. When allowed to react with methanol-*O-d*, the model carbanion is quenched by a fast proton transfer, while the model thiolate ion and the unknown *m/z* 93 ions undergo clustering reactions that are presumably termolecular (e.g., eq 17). The observed cluster ion formation reactions are considerably faster for CH_3S^- than for *m/z* 93.

$$\underset{m/z\ 47}{CH_3S^-} + CH_3OD \xrightarrow{He} \underset{m/z\ 80}{CH_3S^-(DOCH_3)} \qquad (17)$$

---

[19] Unless noted, dipole moments and polarizabilities are obtained from ref 14a.

Table III. Summary of Observations for the Reactions of the *m/z* 93 Ion and Its Models with Various Reagents[a]

reagent	ΔH°_{acid}[b]	CH_3S^-[c]	$CH_3SCH_2^-$[d]	*m/z* 93[e]
N_2O		no reaction	diazotization[f]	no reaction
HCO_2CH_3		no reaction	(transesterification)[g]	no reaction
D_2O	392.8	no reaction	proton transfer and exchange[h]	no reaction
CH_3OD	380.6	cluster	proton transfer	cluster[i]
BuOH	375.0	cluster	(proton transfer)[j]	cluster[i]
t-BuOH	374.6	cluster	(proton transfer)[j]	cluster[i]
CF_3CH_2OH	361.8	cluster	(proton transfer)[j]	cluster
H_2S	351.2	proton transfer	(proton transfer)[j]	no reaction
$CH_2(CO_2Me)_2$	~349	proton transfer	(proton transfer)[j]	no reaction
CH_3CO_2H	348.8	proton transfer	(proton transfer)[j]	proton transfer

[a] The observations reported for any given reagent but for the different ions were collected under identical experimental conditions. Cluster is meant to indicate a termolecular, adduct-forming process (such as that shown in eq 17). [b] Units of kcal mol^{-1}; taken from ref 15. [c] Synthesized by reaction of amide ith methanethiol or as noted in footnote *e*; gas-phase acidity of methanethiol is 356.9 kcal mol^{-1}. [d] Synthesized by reaction of amide with dimethyl sulfide; gas-phase acidity of dimethyl sulfide is 393.2 kcal mol^{-1}. [e] Synthesized by reaction of amide, hydroxide, benzyl anion, and trifluoroethoxide with dimethyl disulfide. The *m/z* 93 anion synthesized in various ways appears to be the same as its further reactivity was independent of method of preparation. [f] See text. [g] Not examined in this work, but transesterification should be rapid by analogy to the chemistry displayed by the allyl anion, ref 21. [h] Four exchanges are observed, but equilibration is the predominant process. [i] Cluster ion formation by *m/z* 93 appears to be significantly slower than that by *m/z* 47. [j] Not examined in this work, but such exothermic proton transfers are know to be fast.

Scheme I. Generalized Scheme for Anions Reacting with Dimethyl Disulfide in the Absence of Solvent and Counterions[a]

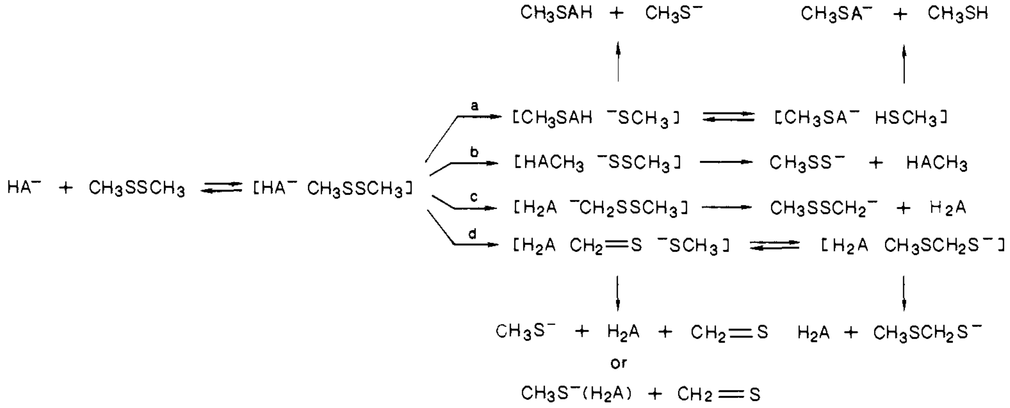

[a] Note that products from direct proton transfer or substitution at carbon (pathways c and b, respectively) were not detected for any of the anions examined.

The model carbanion reacts at a moderate rate with nitrous oxide[2a] by the known diazotization[20,2a] reaction (eq 18), while the

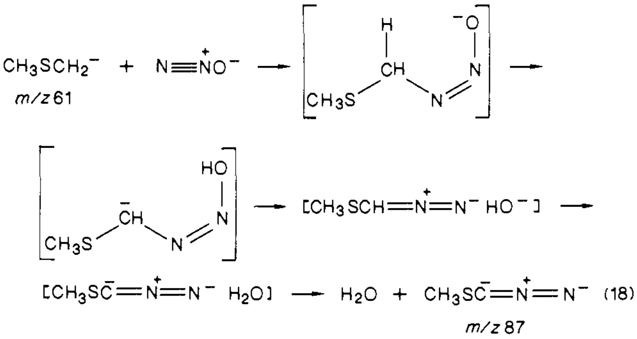

(18)

model thiolate anion and the synthesized *m/z* 93 anion are both unreactive toward nitrous oxide. Finally, neither CH_3S^- nor the unknown *m/z* 93 ion reacts with methyl formate. Methyl formate has been extensively studied with respect to its gas-phase reactions with anions and should readily react with the strongly basic carbanions considered here as it does with the allyl anion among others.[21]

Based on all the observations reported, the *m/z* 93 ion formed in a variety of the anion and dimethyl disulfide reactions is not a primary carbanion! While both the model carbanion and the model thiolate anion will react with H_2S ($\Delta H^\circ_{acid}[H_2S]$ = 351.2 kcal mol^{-1}) by proton transfer, the *m/z* 93 product ion does not react with H_2S, but all three anions do abstract a proton from acetic acid ($\Delta H^\circ_{acid}[CH_3COOH]$ = 348.8 kcal mol^{-1}), which therefore brackets the basicity of the *m/z* 93 anion. While these data clearly discriminate against the *m/z* 93 ion being a carbanion, only indirectly do they support the thiolate structure. Unfortunately, we have not yet found a distinctive reagent uniquely reactive with the thiolate anion as compared to the carbanion. Further confirmation of the assignment of the observed *m/z* 93 ion to a thiolate structure is derived from synthesis[22] of authentic $CH_3SCH_2S^-$, by the exothermic process shown in eq 19.[23] The

$$\underset{m/z\ 61}{CH_3SCH_2^-} + OCS \rightarrow \underset{m/z\ 93}{CH_3SCH_2S^-} + CO + 28 \text{ kcal mol}^{-1} \tag{19}$$

m/z 93 ion synthesized by the route shown in eq 19 displays the same chemical reactivity as the *m/z* 93 ion formed in the dimethyl disulfide reactions discussed above. Therefore we believe that the *m/z* 93 anion observed from dimethyl disulfide reactions is the rearranged thiolate ion $CH_3SCH_2S^-$.

Thermochemistry. In a few of the reactions presented above, and for a variety of the reactions discussed below, we have estimated enthalpy changes using thermochemical data from the literature or values derived from measurements reported here.[24-26]

---

(20) (a) Bierbaum, V. M.; DePuy, C. H.; Shapiro, R. H. *J. Am. Chem. Soc.* **1977**, *99*, 5800–5802. (b) Kass, S. R.; Filley, J.; Van Doren, J. M.; DePuy, C. H. *J. Am. Chem. Soc.* **1986**, *108*, 2849–2852.

(21) DePuy, C. H.; Grabowski, J. J.; Bierbaum, V. M.; Ingemann, S.; Nibbering, N. M. M. *J. Am. Chem. Soc.* **1985**, *107*, 1093–1098.

(22) (a) Bierbaum, V. M.; Grabowski, J. J.; DePuy, C. H. *J. Phys. Chem.* **1984**, *88*, 1389–1393. (b) DePuy, C. H. *Org. Mass Spectrom.* **1985**, *20*, 556–559.

(23) The reaction of the conjugate base of dimethyl sulfide with carbonyl sulfide gives the desired *m/z* 93 ion as the predominant product ion; the two other important product ions are HS^- and $CH_3SCH_2COS^-$ (the adduct ion).

(24) Lias, S. G.; Liebman, J. F.; Levin, R. D. *J. Phys. Chem. Ref. Data* **1984**, *13*, 695–808.

Table IV. Heats of Formation Used in This Work

species	ΔH°_{f298}, kcal mol^{-1}	ref	species	ΔH°_{f298}, kcal mol^{-1}	ref
NH_3	−11	*a*	H_2N^-	26.9	*b*
H_2O	−58	*a*	HO^-	−32.8	*b*
CH_3NH_2	−5	*a*			
CH_3OH	−48	*a*	CH_3O^-	−33.3	*b*
CH_3CN	18	*a*	CH_2CN^-	25.2	*b*
$H_2C{=}CHCH_3$	5	*a*	$H_2C{=}CHCH_2^-$	29.9	*b*
$H_2C{=}S$	24.3	*c*	$H_2C{-}S^-$	13	*d*
CH_3SH	−5.4	*c*	CH_3S^-	−14.3	*b*
CH_3COCH_3	−52	a	$CH_3C(O^-){=}CH_2$	−48.5	*b*
CH_3NO_2	−18	*a*	$CH_2NO_2^-$	−27.2	*b*
CH_3CH_2SH	−11	*c*	$CH_3CH_2S^-$	−21.6	*b*
CH_3SSH	−0.9	*c, e*	CH_3SS^-	−23.5	*e*
$PhCH_3$	12	*a*	$C_6H_5CH_2^-$	27.1	*b*
CH_3SSCH_3	−5.8	*c*			
CH_3SCH_2SH	0.05	*e*	$CH_3SCH_2S^-$	−15.7	*f*

[a] Reference 24. [b] Reference 15. [c] Reference 8a. [d] Reference 25. [e] Calculated from group additivity considerations, ref 8a and 26. [f] Based on the gas-phase acidity reported in the text and the appropriate neutral heat of formation.

The data used in these thermochemical calculations, with the exception of the gas-phase acidities, are collected in Table IV.

Discussion

A generalized reaction scheme for anions reacting with dimethyl disulfide is shown in Scheme I. Chemical reaction is initiated by encounter to form an ion–dipole complex between the anion and dimethyl disulfide. Thermochemical data for ions clustered with dimethyl disulfide have not appeared in the literature,[27] but the interactions should be in the 15–20 kcal mol^{-1} range for this polar solvent molecule (CH_3SSCH_3: $\alpha = 1.05 \times 10^{-23}$ cm^3; $\mu_D = 1.99$ D).[28] The solvation energy in the ion-neutral complex is available to fuel chemical reactions within the complex, or if the complex is sufficiently long-lived, the energy can be removed by a stabilizing collision with a third body, in which case, the cluster ion would be directly observed. In general, three-body cluster ion forming reactions are slow compared to exothermic bimolecular channels. As a result, and as is observed for the systems reported here, exothermic, bimolecular chemical reactions completely overwhelm cluster ion formation under the conditions used (helium buffer gas at a pressure of 0.3 and 0.6 Torr). From the first-formed ion–molecule complex, [HA^- CH_3SSCH_3], there are five chemical processes that should be considered. The trivial pathway of back-dissociation to reactants determines the reaction efficiency,[29] which itself is defined as the fraction of collisions that lead to product formation. While we have not accurately measured rate coefficients for these systems,[30] qualitatively it is apparent that many of the reactions are fast, having efficiencies greater than 10%, and that the slowest reactions are those of the weakest bases. A second pathway (Scheme I, path c) from the initial ion–molecule complex involves proton transfer to give a new ion–molecule complex consisting of a stable primary carbanion solvated by the newly formed protonated base; such a complex could dissociate to give a $(C_2H_5S_2)^-$ product ion at *m/z* 93. While proton transfer is quantitatively observed for strongly basic anions with dimethyl sulfide, direct proton transfer to give an observable primary carbanion is not evident in our studies on dimethyl disulfide. Indeed, we are able to explain all the data presented in this paper without recourse to a primary carbanion as a reaction intermediate. The absence of evidence of a stable conjugate base to dimethyl disulfide may imply that it is inappropriate to consider dimethyl disulfide as a normal Brønsted acid.

For Scheme I, there remain three chemically significant reaction channels to be discussed. The first is S_N2 displacement at carbon to yield the methyl disulfide anion, CH_3SS^-, *m/z* 79 (Scheme I, path b). The S_N2 reaction at carbon center is well studied in the gas phase and has been shown to occur, albeit slowly, for leaving groups more basic than CH_3SS^- (e.g., F^- where $\Delta H^\circ_{acid}[HF] = 371.5$ kcal mol^{-1}). Displacement at carbon has not been detected however for either dimethyl ether ($\Delta H^\circ_{acid}[CH_3OH] = 380.6$ kcal mol^{-1}) or dimethyl sulfide ($\Delta H^\circ_{acid}[CH_3SH] = 356.9$ kcal mol^{-1}), and from the data herein, it does not routinely occur for dimethyl disulfide. The gas-phase acidity of CH_3SSH has recently become available based on Moran and Ellison's measurement of the electron binding energy of CH_3SS^- by negative ion photoelectron spectroscopy,[1] $\Delta H^\circ_{acid}(CH_3SSH) = 343.1$ kcal mol^{-1}. Using the acidity of methyl hydrogen disulfide and other thermochemical values from Table IV, we estimate that the S_N2 reaction at carbon between amide and dimethyl disulfide is exothermic by 50 kcal mol^{-1}. In spite of the large reaction exothermicity for the amide reaction, a carbon-based S_N2 reaction involving dimethyl disulfide does not occur. Indeed, for none of the anions examined was a carbon-centered nucleophilic displacement reaction observed. The lack of observation of the carbon-center displacement channel is a combination of (an expected) slow carbon substitution process and the availability of fast competing processes. However, the observations on the sulfur nucleophiles with dimethyl disulfide imply that carbon-centered substitution must have a high kinetic barrier. For the reaction of thioethoxide with dimethyl disulfide, elimination is not observed, and understandably so, since we estimate that the initial step is quite endothermic (eq 20a). For the same reaction the sulfur substitution process is slightly endothermic (eq 20b), while the carbon-centered substitution reaction is reasonably exothermic (eq 20c). Yet the slightly endothermic sulfur substitution reaction is the major (and probably exclusive) reaction, albeit with a relatively low efficiency!

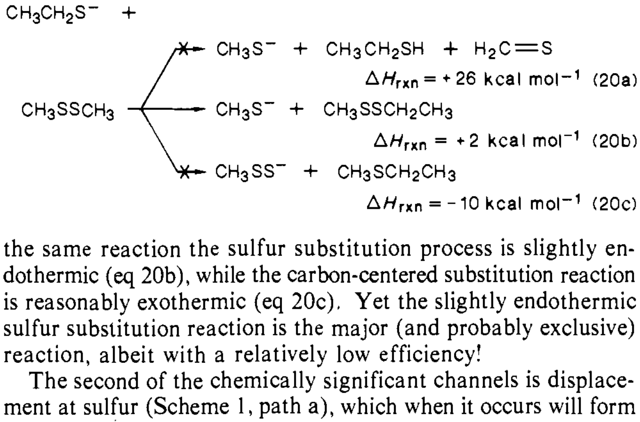

The second of the chemically significant channels is displacement at sulfur (Scheme 1, path a), which when it occurs will form an ion–dipole complex between methanethiolate and the newly formed sulfur-containing neutral [CH_3SAH $^-SCH_3$]. This ion–dipole complex can either dissociate to give methanethiolate and the thiomethoxylated nucleophile or, depending upon the acidity of the newly formed sulfur-containing molecule, undergo an intermolecular proton transfer within the ion–dipole complex followed by dissociation, yielding the thiomethoxylated anion and methanethiol (e.g., reactions 9 and 11).

The final chemically significant channel in Scheme I is an elimination process across the carbon–sulfur bond to form an ion–molecule complex between three species, the newly formed neutral base, thioformaldehyde, and methanethiolate (Scheme I, path d). Partitioning from this ion–molecule complex can proceed in one of three directions, the first of which is simple dissociation to yield methanethiolate ion and two neutrals. Because the complex formed in the elimination channel is a ternary complex, the second direction is dissociation into a solvated anion and neutral thioformaldehyde. Finally, the ternary complex formed in path d of Scheme I contains a nucleophile and a highly reactive

---

(25) Moran, S.; Ellison, G. B. *Int. J. Mass Spectrom. Ion Processes* **1987**, *80*, 83–98.

(26) Benson, S. W. *Thermochemical Kinetics*, 2nd ed.; Wiley-Interscience: New York, 1976.

(27) Keesee, R. G.; Castleman, A. W., Jr. *J. Phys. Chem. Ref. Data* **1986**, *15*, 1011–1071.

(28) (a) Polarizability estimated from the method of: Miller, K. J.; Savchik, J. A. *J. Am. Chem. Soc.* **1979**, *101*, 7206–7213. (b) Dipole moment from: Abraham, R. J.; Hudson, B. *J. Comput. Chem.* **1984**, *5*, 562–570.

(29) Reaction efficiency is defined as the observed bimolecular rate coefficient divided by the collision rate coefficient, where the collision rate coefficient is calculated according to ref 16.

(30) For hydroxide, we[18] estimate $k_{II} = 2.8 \times 10^{-9}$ cm^3 molecule^{-1} s^{-1}, $k_{coll} = 3.3 \times 10^{-9}$ cm^3 molecule^{-1} s^{-1}, and Eff = 0.85 (from two measurements of *k*); while for thioethoxide, we estimate $k_{II} = 6 \times 10^{-12}$ cm^3 molecule^{-1} s^{-1}, $k_{coll} = 1.76 \times 10^{-9}$ cm^3 molecule^{-1} s^{-1}, and Eff = 0.003 (from one measurement of *k*). The collision rate coefficients are calculated according to ref 16.

electrophile such that addition of one to the other and then separation into the rearranged thiolate ion and the conjugate acid of the starting base can take place. It is important to note that formation of the solvated ion and the rearranged thiolate ion is dependent on the existence of an additional particle to carry off the reaction exothermicity. Using our estimated proton affinity of the rearranged thiolate ion and other thermochemical values in Table IV, we approximate the C–S bond formed when methanethiolate adds to thioformaldehyde to be worth ~26 kcal mol^{-1}. The formation of the rearranged thiolate ion could, in principle, also take place by the Wittig rearrangement.[31] Such a process is very similar to that shown except the "extra electron" in the ternary complex shown in path d, Scheme I would formally reside on the thioformaldehyde. For none of the systems did we detect the known, stable thioformaldehyde molecular anion, whereas we did find the solvated ions shown in Tables I and II. Furthermore, we have been unable to uncover any evidence of a stable carbanion corresponding to deprotonated dimethyl disulfide (and which would be an intermediate on the Wittig rearrangement surface). Even in the reaction of amide with dimethyl-d_6 disulfide was no evidence found for H/D exchange in the products.[18] Thus we prefer the elimination rearrangement process shown in Scheme I rather than the similar Wittig rearrangement.

From the data reported in Results for the reaction of amide ion with dimethyl disulfide in light of Scheme I, it is obvious that at least 67% of the reaction is proceeding by the elimination channel as evidenced by that amount of $CH_3SCH_2S^-$ formed. The 33% of methanethiolate formed could come from either the elimination or displacement channels (Scheme I, pathways d and a, respectively; eq 21). Products from direct proton transfer or substitution at carbon are not detected (Scheme I, pathways c and b, respectively).

$$H_2N^- + CH_3SSCH_3 \longrightarrow 33\%\ CH_3S^- + [CH_3SNH_2 \text{ and/or } H_2C{=}S + NH_3] \tag{21a}$$
$$\longrightarrow 67\%\ CH_3SCH_2S^- + NH_3 \tag{21b}$$

Compare the amide results to those from methoxide in which 77% of the reaction proceeds to form the rearranged thiolate ion, 11% the methanol-solvated methanethiolate and 12% methanethiolate itself. Thus, methoxide with dimethyl disulfide goes at least 88% of the time by way of the elimination channel. The 12% of methanethiolate formed could come from either the elimination or displacement channels. Incidentally, the high yield of the m/z 93 ion in the methoxide reaction was the first clue that the m/z 93 ion might not be the primary carbanion—it appeared to be unlikely to us that methoxide could be a strong enough base to deprotonate dimethyl disulfide.

$$CH_3O^- + CH_3SSCH_3 \longrightarrow 12\%\ CH_3S^- + [CH_3SOCH_3 \text{ and/or } H_2C{=}S + CH_3OH] \tag{22a}$$
$$\longrightarrow 11\%\ CH_3S^-(CH_3OH) + H_2C{=}S \tag{22b}$$
$$\longrightarrow 77\%\ CH_3SCH_2S^- + CH_3OH \tag{22c}$$

Hydroxide ion, which is intermediate to methoxide and amide in base strength, gives roughly similar results (eq 23). The 3% of CH_3SO^- found must come from path a in Scheme I, nucleophilic displacement at sulfur followed by intermolecular proton transfer within the ion–molecule complex. The latter product has been carefully checked; upon using perdeuterated dimethyl disulfide, the ion in question shifted to 3 mass units higher and was formed in the same amount.[18]

$$HO^- + CH_3SSCH_3 \longrightarrow 33\%\ CH_3S^- + [CH_3SOH \text{ and/or } H_2C{=}S + H_2O] \tag{23a}$$
$$\longrightarrow 3\%\ CH_3SO^- + CH_3SH \tag{23b}$$
$$\longrightarrow 6\%\ CH_3S^-(H_2O) + H_2C{=}S \tag{23c}$$
$$\longrightarrow 58\%\ CH_3SCH_2S^- + H_2O \tag{23d}$$

The data for the three anions for which the charge is localized are consistent with predominant reaction by way of the elimination channel. While the absolute rate coefficients are not yet available, all three anions (amide, hydroxide, methoxide) show a high degree of reaction efficiency with dimethyl disulfide (it appears that greater than 40% of the ion–dimethyl disulfide collisions lead to product formation).[30] In contrast, displacement reactions at carbon show a marked sensitivity to reaction exothermicity.[32] The qualitative similarity in reaction rate coefficients is also in accord with an interpretation in which most of the reaction (for amide, hydroxide, and methoxide with dimethyl disulfide) proceeds by elimination across the sulfur–carbon bond. For the weakest of these three bases, the ternary ion–molecule complex, [H_2A $H_2C{=}S$ $^-SCH_3$], postulated as an intermediate on the reaction coordinate, will contain the smallest amount of energy, with the implication that it should live longer (i.e., the density of states at the reaction energy, over the productive reaction and/or dissociation barriers, will be smaller than that present when a stronger base induces the chemical processes). The longer lifetimes will increase the probability of further reaction within the product ion–dipole complex (e.g., readdition of methanethiolate to thioformaldehyde). The smaller the amount of excess energy in the ternary complex formed in the elimination channel, the higher the probability that the solvated ion will remain together when the complex dissociates (i.e., the less exothermicity will be available to "boil off" the solvent). It is also apparent that a portion of the observed methanethiolate signal is probably due to sulfur substitution (i.e., eq 23b) but that sulfur substitution is significantly less important than elimination.

Next, consider the reactions of the delocalized anions with dimethyl disulfide. The conjugate base of nitromethane yields only the sulfur-containing anion as shown in eq 13. The observation of a single product from nitromethide indicates that exclusive displacement at sulfur has occured, followed by an intermolecular proton transfer within the product ion–dipole complex (Scheme I, path a). Dimethyl sulfide is 23.4 kcal mol^{-1} more acidic than methane, which to a first approximation would indicate that $CH_3SCH_2NO_2$ should be 23 kcal mol^{-1} more acidic (and probably something less due to the saturation effect)[15b] than nitromethane. The final intermolecular proton transfer within the ion–dipole complex (i.e., final step of path d in Scheme I) should be exothermic by about 24 kcal mol^{-1} (or slightly less; this estimate neglects differences in solvation energies of the two complexes[33]). We are unable to estimate the reaction exothermicity for the direct sulfur substitution process, but based on the similar proton affinities of methanethiolate and nitromethide, the displacement reaction is close to thermoneutral such that it is reasonable for the product ion–dipole complex to have sufficient lifetime to be completely converted into the thermodynamically favored acid–base pair (Scheme II). As with the thioethoxide reaction discussed above, it is not surprising that elimination products are not observed in the reaction of nitromethide with dimethyl disulfide, even though formation of the rearranged thiolate product ion is energetically allowed. The initial step of the elimination is endothermic by 25 kcal mol^{-1} (eq 24).

$$CH_2NO_2^- + CH_3SSCH_3 \longrightarrow 0\%\ CH_3S^- + H_2C{=}S + CH_3NO_2 \quad \Delta H_{rxn} = +25 \text{ kcal mol}^{-1} \tag{24a}$$
$$\longrightarrow 0\%\ CH_3SCH_2S^- + CH_3NO_2 \quad \Delta H_{rxn} = -1 \text{ kcal mol}^{-1} \tag{24b}$$
$$\longrightarrow 100\%\ CH_3SCHNO_2^- + CH_3SH \tag{24c}$$

The results for acetone enolate are similar to those for nitromethide; the predominant product is the sulfur-containing ion, but now a minor product appears, methanethiolate. From simple acidity comparisons analogous to those discussed above, $CH_3COCH_2SCH_3$ should be no more than 10 kcal mol^{-1} more acidic

---

(31) Schollkopf, U. *Angew. Chem., Int. Ed. Engl.* **1970**, *9*, 763–773.

(32) Damrauer, R.; DePuy, C. H.; Bierbaum, V. M. *Organometallics* **1982**, *1*, 1553–1554.

(33) Grabowski, J. J.; DePuy, C. H.; Bierbaum, V. M. *J. Am. Chem. Soc.* **1983**, *105*, 2565–2571.

Scheme II

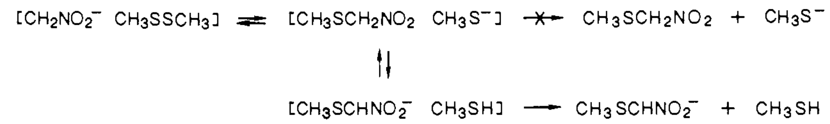

$$\begin{aligned}&[CH_2NO_2^- \; CH_3SSCH_3] \rightleftharpoons [CH_3SCH_2NO_2 \; CH_3S^-] \not\rightarrow CH_3SCH_2NO_2 + CH_3S^- \\ &\qquad\qquad\qquad\qquad\qquad\qquad \upharpoonleft\downharpoonright \\ &\qquad\qquad\qquad\qquad [CH_3SCHNO_2^- \; CH_3SH] \rightarrow CH_3SCHNO_2^- + CH_3SH\end{aligned}$$

than methanethiol. The absence of the elimination channel, again evidenced by the lack of the rearranged thiolate product ion *m/z* 93, and the endothermicity of formation of methanethiolate by elimination (channel 25a) are taken to mean that the acetone enolate ion reacts with dimethyl disulfide exclusively by substitution at sulfur. Even though our estimates place channel 25d as being more exothermic than channel 25c (i.e., $CH_3COCH_2SCH_3$ is estimated to be more acidic than CH_3SH), 21% of the less thermodynamically favored product is observed *and the only difference between the two observed channels is an exothermic proton transfer.* The incomplete proton equilibration in the acetone system (whereas complete equilibration was observed in the nitromethane system, Scheme II) is a reflection of the smaller exothermicity of the final proton-transfer step and the greater exothermicity of the initial sulfur substitution step (the larger the exothermicity in the sulfur substitution step, the shorter the lifetime of the initial product ion–dipole complex and the less opportunity there is for the final proton transfer).

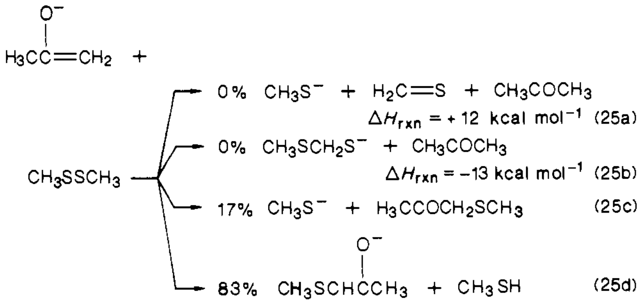

$$\begin{aligned}&H_3C\overset{O^-}{\overset{|}{C}}{=}CH_2 + CH_3SSCH_3 \rightarrow \\ &\quad 0\%\ CH_3S^- + H_2C{=}S + CH_3COCH_3 \qquad \Delta H_{rxn} = +12\ \text{kcal mol}^{-1} \quad (25a) \\ &\quad 0\%\ CH_3SCH_2S^- + CH_3COCH_3 \qquad \Delta H_{rxn} = -13\ \text{kcal mol}^{-1} \quad (25b) \\ &\quad 17\%\ CH_3S^- + H_3CCOCH_2SCH_3 \quad (25c) \\ &\quad 83\%\ CH_3SCH\overset{O^-}{\overset{|}{C}}CH_3 + CH_3SH \quad (25d)\end{aligned}$$

A similar interpretation to that expressed above for nitromethane and acetone accounts for the data from the reaction of the conjugate base of acetonitrile with dimethyl disulfide. For this latter case, a slightly larger percentage of the reaction proceeds to yield methanethiolate (eq 26). The first step of the elimination is still endothermic (but by only a fraction of the available ion–dipole complex solvation energy) and apparently presents enough of a kinetic barrier so as to preclude formation of the rearranged thiolate ion, a channel estimated to be exothermic with respect to reactants by 13 kcal mol^{-1}. A simple additivity scheme predicts $\Delta H°_{acid}(CH_3SCH_2CN) \geq 351$ kcal mol^{-1}, whereas $\Delta H°_{acid}(CH_3SH) = 356.9$ kcal mol^{-1}. Comparing nitromethide, acetone enolate, and cyanomethide, the extent of proton equilibration increases as the anion base is made weaker and weaker. This is presumably due to a combination of two effects; less exothermicity in the initial sulfur substitution step, which results in a longer product ion–dipole complex lifetime, and a more exothermic, and therefore a more favorable, proton transfer within the product ion–dipole complex.

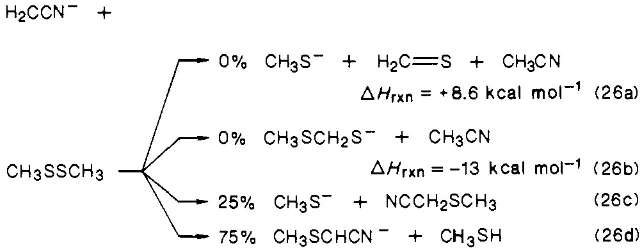

$$\begin{aligned}&H_2CCN^- + CH_3SSCH_3 \rightarrow \\ &\quad 0\%\ CH_3S^- + H_2C{=}S + CH_3CN \qquad \Delta H_{rxn} = +8.6\ \text{kcal mol}^{-1} \quad (26a) \\ &\quad 0\%\ CH_3SCH_2S^- + CH_3CN \qquad \Delta H_{rxn} = -13\ \text{kcal mol}^{-1} \quad (26b) \\ &\quad 25\%\ CH_3S^- + NCCH_2SCH_3 \quad (26c) \\ &\quad 75\%\ CH_3SCHCN^- + CH_3SH \quad (26d)\end{aligned}$$

The conjugate base of ethylbenzene gives almost exclusively methanethiolate (eq 27) and just a trace amount of the rearranged thiolate ion. As we proceeded from the weakest of the delocalized carbanions (nitromethide) to the present point, we found a smooth increase in the relative yield of methanethiolate. Our additivity estimates show that $\Delta H°_{acid}[PhCH(CH_3)SCH_3] \geq 357$ kcal mol^{-1}, which is to say that this new compound is probably somewhat less acidic than methanethiol and that the final step of path d in Scheme I is *endothermic.*

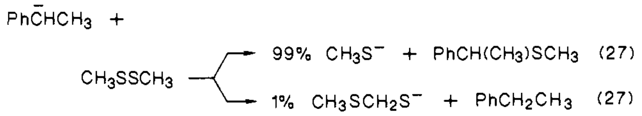

$$\begin{aligned}&Ph\bar{C}HCH_3 + CH_3SSCH_3 \rightarrow \\ &\quad 99\%\ CH_3S^- + PhCH(CH_3)SCH_3 \quad (27) \\ &\quad 1\%\ CH_3SCH_2S^- + PhCH_2CH_3 \quad (27)\end{aligned}$$

The allyl anion gives results similar to that found for the benzyl anions; reaction is observed to give predominantly methanethiolate. The various channels and their exothermicities are summarized in eq 28. In order to decide by which route the methanethiolate is formed in the allyl anion reaction, compare the data for allyl to that for hydroxide. These latter two anions have equivalent thermodynamic basicities in the gas phase yet give strikingly different product yields when allowed to react with dimethyl disulfide. Such a distinction implies substantially different hypersurfaces for the reactions. We interpret these differences to indicate that allyl anion gives predominantly methanethiolate by substitution at sulfur and only a small percentage of the overall reaction goes by the elimination route. On the other hand, hydroxide goes predominatly by the elimination route and only a small percentage by substitution at sulfur. Thus for equivalent thermodynamic bases, different reactivities are seen based upon differences in the type of anionic nucleophile. These observations are in accord with preferences predicted by hard–soft acid/base theory. The observation of only trace amounts of the rearranged thiolate ion from both allyl and benzyl anions indicates that elimination must be the minor path and therefore that the methanethiolate anion is being produced by a sulfur substitution process. The contrast between anions of like thermodynamic basicity yet opposite kinetic behavior observed for the hydroxide/allyl anion pair is also found for methoxide/benzyl anion.

Some of the reactions presented in Results have product channels that yield cluster ions, such as $CH_3S^-(H_2O)$. While we can reproducibly measure a yield of the clustered product ion (at a given bath gas pressure), it is possible that we are in fact detecting only a fraction of the initially formed cluster ions as the cluster ion while the remaining fraction is detected as the unsolvated ion (e.g., CH_3S^-). Hierl and co-workers[34] have shown that even for cluster ions with bond dissociation energies of 13–15 kcal mol^{-1} thermal collisions with the buffer gas can cause collisionally activated dissociation (CAD) on the time scale of detection in the FA. Thus it is possible that some fraction of the CH_3S^- we detect in the amide, hydroxide, and methoxide reactions was actually produced as the appropriate cluster ion, which then underwent thermally activated CAD in a subsequent step. The CAD step will only be related to the reaction of interest by the fraction of the reaction exothermicity deposited in internal degrees of freedom in the clustered ion. CAD by room-temperature processes are anticipated to be more important for the weaker bound cluster ions and perhaps for the more exothermic reactions. Thus, the lack of observation of a $CH_3S^-(NH_3)$ cluster ion may be due to CAD, as the bond in this species is anticipated to be fairly weak (for example, the enthalpy required to dissociate Br^- from NH_3 is only 7.7 kcal mol^{-1}).[27] If CAD of $CH_3S^-(NH_3)$ is indeed occurring in the amide, hydroxide, or methoxide reactions, our interpretation that most of the reaction is proceeding by way of the elimination route is strengthened as the cluster ion must be due to that channel.

---

[34] Hierl, P. M.; Ahrens, A. F.; Henchman, M.; Viggiano, A. A.; Paulson, J. F. *Int. J. Mass Spectrom. Ion Processes* **1987**, *81*, 101–122.

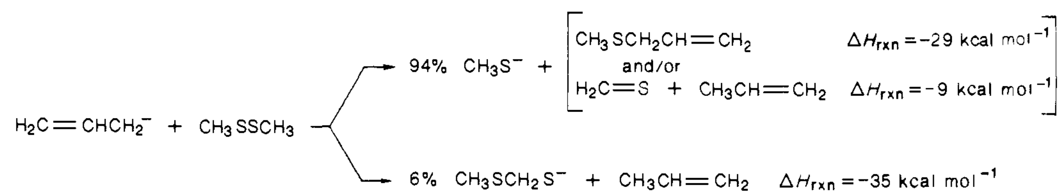

$$H_2C{=}CHCH_2^- + CH_3SSCH_3 \rightarrow 94\%\ CH_3S^- + \left[\begin{array}{ll} CH_3SCH_2CH{=}CH_2 & \Delta H_{rxn} = -29\ \text{kcal mol}^{-1} \\ \quad \text{and/or} & \\ H_2C{=}S + CH_3CH{=}CH_2 & \Delta H_{rxn} = -9\ \text{kcal mol}^{-1} \end{array}\right] \tag{28a}$$

$$H_2C{=}CHCH_2^- + CH_3SSCH_3 \rightarrow 6\%\ CH_3SCH_2S^- + CH_3CH{=}CH_2 \quad \Delta H_{rxn} = -35\ \text{kcal mol}^{-1} \tag{28b}$$

Conclusions

A variety of anions were found to react with dimethyl disulfide, including all anions examined that are more basic than methanethiolate. In addition, sulfur nucleophiles slightly less basic than thiomethoxide were observed to undergo slow thiolate/disulfide interchange reactions with dimethyl disulfide, but anions less basic than HS^- reacted too slowly to give observed reaction products. Two bimolecular reaction pathways were found to account for all the primary reaction products: substitution at sulfur and elimination across the carbon-sulfur bond. Each of these two pathways can give more than one subsequent ion product. No evidence was found for an ion that would correspond to deprotonated dimethyl disulfide, and no evidence was found for carbon-centered substitution processes in the reactions examined. Nucleophilic displacement is thus an easier process at sulfur centers as compared to carbon centers. The primary factor in determining whether an anion gave sulfur substitution products or elimination products is the structure of the anion and not the energetics. Anionic bases of similar base strength (and similar reaction energetics), but of dissimilar structures, gave markedly different product distributions. Anions at least as basic as methoxide and in which the charge is localized preferred to react by elimination, while delocalized carbanions of similar basicity strongly preferred substitution at sulfur (e.g., compare hydroxide to allyl anion and methoxide to benzyl anion). With anions less basic than methoxide, no evidence was found for elimination, which was interpreted to be due to the energetically unfavorable initial proton abstraction, even though the ultimate product (the rearranged thiolate ion) was exothermic or at least thermoneutral with respect to starting materials. Thus, when considering the competition between elimination and substitution, one needs to consider additional factors besides energetics. Hydroxide prefers elimination while allyl anion prefers substitution, at least in the reactions of dimethyl disulfide. These data on the intrinsic reactivity of anions with a model disulfide provide clear new insight into the fundamental chemical behavior of molecules containing sulfur-sulfur linkages.

Acknowledgment. We gratefully acknowledge financial support of this work by a National Science Foundation Presidential Young Investigator Award (Grant CHE-8552742).

Registry No. Me_2S, 624-92-0; H_2N^-, 17655-31-1; HO^-, 14280-30-9; $CH_2{=}CHCH_2^-$, 1724-46-5; CH_3O^-, 3315-60-4; PhC^-HCH_3, 13822-53-2; $CH_3COCH_2^-$, 24262-31-5; $CH_2NO_2^-$, 18137-96-7; CH_2CN^-, 21438-99-3.

Gas-Phase Ion-Molecule Reactions of the Nitric Oxide Anion

Elizabeth Rinden,[†] **M. Matti Maricq,**[*,†] **and Joseph J. Grabowski**[*,‡]

Contribution from the Departments of Chemistry, Brown University, Providence, Rhode Island 02912, and Harvard University, Cambridge, Massachusetts 02138.

Received June 28, 1988

Abstract: The chemical reactivity of nitric oxide anion (NO^-) with a variety of organic neutrals at ambient energies and in argon bath gas has been probed using the flowing afterglow technique. The reactions fall into four main classes: electron transfer, dissociative electron transfer and/or displacement, collisional detachment, and clustering. Electron transfer can occur when the neutral reactant possesses a positive electron affinity greater than the electron affinity of $NO^\bullet$, but does not always do so. Bimolecular substitution at sulfur is shown to occur with dimethyl disulfide, but for other substrates, distinguishing between displacement and dissociative electron transfer is not possible. Collisional detachment is the exclusive reaction channel observed for a few of the molecules examined and occurs to some extent with many of the neutrals tested. Cluster ion formation between NO^- and a number of the reactant neutrals which possess permanent dipole moments is observed. Additional pathways were observed for several of the neutrals examined. The collected observations are discussed in light of the general theory of ion-molecule reactions.

Nitric oxide has one of the smallest positive electron affinities known[1] (EA[$NO^\bullet$] = 0.024 eV or 0.55 kcal/mol). The binding energy of NO^- is so small that a significant fraction of the thermal collisions with gas molecules at room temperature contains sufficient energy to detach an electron.[2] Even though the rate coefficient for collisional detachment of NO^- by helium is small[3] ($k_{obs} = 2.4 \times 10^{-13}$ cm^3/s; $k_{obs}/k_{coll} = 0.0004$), there are enough collisions between NO^- and the helium present at 0.3 Torr in most flowing afterglow (FA) experiments to ensure that the net probability of collisional detachment is near unity.

A number of years ago, Fehsenfeld and co-workers[4] discovered that when argon is used in place of helium in a flowing afterglow, a significant fraction of the NO^- ions survive the viscous flow through the reaction region of the apparatus and are readily detected. McFarland and colleagues[3] took advantage of the

---

[†] Brown University.

[‡] Harvard University.

[1] (a) Siegel, M. W.; Celotta, R. J.; Hall, J. L.; Bennett, R. A. *Phys. Rev.* **1972**, *A6*, 607. (b) Drziac, P. S.; Marks, J.; Brauman, J. I. In *Gas Phase Ion Chemistry*; Bowers, M. T., Ed.; Academic Press: Orlando, FL, 1984; Vol. 3, Chapter 21. (c) Mead, R. D.; Stevens, A. E.; Lineberger, W. C. In *Gas Phase Ion Chemistry*; Bowers, M. T., Ed.; Academic Press: Orlando, FL, 1984; Vol. 3, Chapter 22.

[2] The electron binding energy of nitric oxide is less than kT at room temperature; at 300 K, kT = 208.5 cm^{-1}, whereas 0.024 eV is equivalent to 193.6 cm^{-1}.

[3] McFarland, M.; Dunkin, D. B.; Fehsenfeld, F. C.; Schmeltekopf, A. L.; Ferguson, E. E. *J. Chem. Phys.* **1972**, *56*, 2358-2364.

[4] Fehsenfeld, F. C.; Ferguson, E. E.; Schmeltekopf, A. L. *J. Chem. Phys.* **1966**, *45*, 1844-1845.

0002-7863/89/1511-1203$01.50/0